$Zn_2(VO_4)(IO_3)$: A Novel Polar Zinc(II) Vanadium(V) Iodate With A Large SHG Response

*Bing-Ping Yang, Chun-Li Hu, Xiang Xu, Chao Huang and Jiang-Gao Mao**

Supporting Information

Table S1. Selected bond angles (°) for $Zn_2(VO_4)(IO_3)$.

Table S2. Calculation of dipole moment for IO_3, ZnO_6, ZnO_5, VO_4 polyhedra and net dipole moment for a unit cell in $Zn_2(VO_4)(IO_3)$ (D = Debyes).

Table S3. The state energies (eV) of the highest valence band (H-VB) and the lowest conduction band (L-CB) of the crystal $Zn_2(VO_4)(IO_3)$.

Figure S1. Interconnections of ZnO_n and IO_3 polyhedra (a), interconnections of ZnO_n and VO_4 polyhedra (b). $Zn(1)O_5$ trigonal bipyramids and $Zn(2)O_6$ octahedra are shaded in blue and turquoise, respectively.

Figure S2. Experimental and simulated powder X-ray diffraction data for $Zn_2(VO_4)(IO_3)$.

Figure S3. Infrared spectrum for $Zn_2(VO_4)(IO_3)$.

Figure S4. UV-Vis absorption spectrum for $Zn_2(VO_4)(IO_3)$.

Figure S5. Calculated band structures of $Zn_2(VO_4)(IO_3)$ (the Fermi level is set at 0 eV).

Figure S6. Total and partial electronic density of states of $Zn_2(VO_4)(IO_3)$.

Figure S7. The imaginary and real parts of the dielectric function polarized along three dielectric axes directions (a and b) and the average imaginary part and real part of the dielectric function over three dielectric axes directions (c) for $Zn_2(VO_4)(IO_3)$.

Figure S8. Calculated linear refractive indices for $Zn_2(VO_4)(IO_3)$.

Figure S9. The calculated macroscopic dipole moment vector for compound $Zn_2(VO_4)(IO_3)$ (D = Debyes).

Table S1 Selected bond angles (°) for $Zn_2(VO_4)(IO_3)$.

O(11)-Zn(1)-O(3)#1	130.2(3)	O(1)#3-Zn(2)-O(13)#3	108.0(3)
O(11)-Zn(1)-O(4)	117.8(3)	O(1)#3-Zn(2)-O(12)#4	90.4(3)
O(3)#1-Zn(1)-O(4)	110.8(3)	O(13)#3-Zn(2)-O(12)#4	92.7(2)
O(11)-Zn(1)-O(3)	98.2(3)	O(1)#3-Zn(2)-O(11)	93.4(3)
O(3)#1-Zn(1)-O(3)	95.5(3)	O(13)#3-Zn(2)-O(11)	152.0(2)
O(4)-Zn(1)-O(3)	85.3(2)	O(12)#4-Zn(2)-O(11)	105.3(2)
O(11)-Zn(1)-O(4)#1	88.4(3)	O(1)#3-Zn(2)-O(12)	160.4(2)
O(3)#1-Zn(1)-O(4)#1	84.1(2)	O(13)#3-Zn(2)-O(12)	90.3(2)
O(4)-Zn(1)-O(4)#1	87.0(2)	O(12)#4-Zn(2)-O(12)	81.64(12)
O(3)-Zn(1)-O(4)#1	171.6(3)	O(11)-Zn(2)-O(12)	71.8(2)
O(1)-V(1)-O(4)#6	108.6(3)	O(1)#3-Zn(2)-O(2)#5	97.0(3)
O(1)-V(1)-O(3)	110.8(3)	O(13)#3-Zn(2)-O(2)#5	76.6(2)
O(4)#6-V(1)-O(3)	114.2(3)	O(12)#4-Zn(2)-O(2)#5	168.4(2)
O(1)-V(1)-O(2)	107.4(4)	O(11)-Zn(2)-O(2)#5	83.3(2)
O(4)#6-V(1)-O(2)	107.3(3)	O(12)-Zn(2)-O(2)#5	94.0(2)
O(3)-V(1)-O(2)	108.3(3)	O(13)-I(1)-O(11)	96.4(3)
O(13)-I(1)-O(2)#7	80.8(3)	O(13)-I(1)-O(12)	90.7(3)
O(11)-I(1)-O(2)#7	85.4(2)	O(11)-I(1)-O(12)	86.7(3)
O(12)-I(1)-O(2)#7	167.6(3)		
Zn(1)#2-O(3)-Zn(1)	95.5(3)	Zn(1)-O(4)-Zn(1)#2	93.8(2)
Zn(1)-O(11)-Zn(2)	124.0(3)	Zn(2)#12-O(12)-Zn(2)	130.2(3)
V(1)-O(1)-Zn(2)#8	159.3(4)	V(1)-O(2)-Zn(2)#9	130.2(3)
V(1)-O(3)-Zn(1)#2	125.0(4)	V(1)-O(3)-Zn(1)	139.2(4)
V(1)#11-O(4)-Zn(1)	130.2(4)	V(1)#11-O(4)-Zn(1)#2	127.3(3)
I(1)-O(11)-Zn(1)	129.2(3)	I(1)-O(11)-Zn(2)	101.6(3)
I(1)-O(12)-Zn(2)#12	126.6(3)	I(1)-O(12)-Zn(2)	99.9(3)
I(1)-O(13)-Zn(2)#8	111.9(3)		

Symmetry transformations used to generate equivalent atoms: #1 x, -y+1, z+1/2; #2 x, -y+1, z-1/2; #3 x+1, y, z; #4 x, -y+2, z-1/2; #5 x+1, y, z+1; #6 x-1, -y+1, z-1/2; #7 x, y, z+1; #8 x-1, y, z; #9 x-1, y, z-1; #10 x, y, z-1; #11 x+1, -y+1, z+1/2; #12 x, -y+2, z+1/2.

Table S2. Calculation of dipole moment for IO_3, ZnO_6, ZnO_5, VO_4 polyhedra and net dipole moment for a unit cell in $Zn_2(VO_4)(IO_3)$ (D = Debyes).

$Zn_2(VO_4)(IO_3)$ (Z = 2)				
Polar unit (a unit cell)	Dipole moment (D)			
	x-component	y-component	*z*-component	total magnitude
IO_3	6.043674967	-5.43944	-14.8672	16.94545
	6.043654865	5.439315	-14.8671	16.94532
ZnO_6	-0.603396147	1.071935	2.301066	2.609221
	-0.603561645	-1.0719	2.300968	2.609158
ZnO_5	2.018369277	-1.36626	-0.71147	2.539027
	2.01826008	1.366327	-0.71136	2.538947
VO_4	-0.909799716	2.60281	-0.49807	2.801862
	-0.909915945	-2.6027	-0.49807	2.801799
Net dipole moment	13.09728574	0	-27.5513	30.51
Cell Volume	285.8 $Å^3$			

Table S3. The state energies (eV) of the highest valence band (H-VB) and the lowest conduction band (L-CB) of the crystal $Zn_2(VO_4)(IO_3)$.

Compound	k-point	H-VB	L-CB
$Zn_2(VO_4)(IO_3)$	Z (0.000, 0.000, 0.500)	-0.26316	3.19116
	G (0.000, 0.000, 0.000)	-0.10011	2.74104
	Y (0.000, 0.500, 0.000)	-0.00005	2.70447
	A (-0.500, 0.500, 0.000)	0	2.73605
	B (-0.500, 0.000, 0.000)	-0.01875	2.80005
	D (-0.500, 0.000, 0.500)	-0.36018	3.29278
	E (-0.500, 0.500, 0.500)	-0.32275	3.26668
	C (0.000, 0.500, 0.500)	-0.28764	3.12957

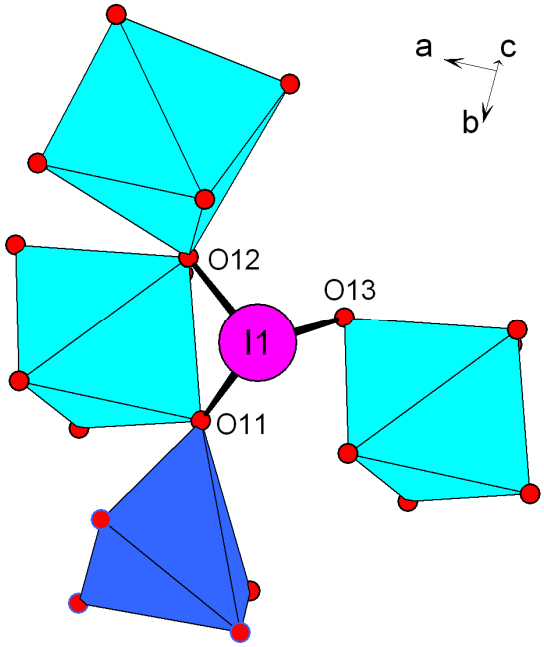

(a)

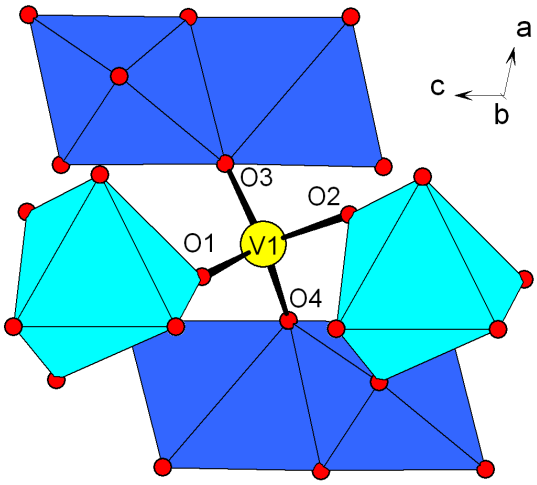

(b)

Figure S1. Interconnections of ZnO_n and IO_3 polyhedra (a), Interconnections of ZnO_n and VO_4 polyhedra (b). $Zn(1)O_5$ trigonal bipyramids and $Zn(2)O_6$ octahedra are shaded in blue and turquoise, respectively.

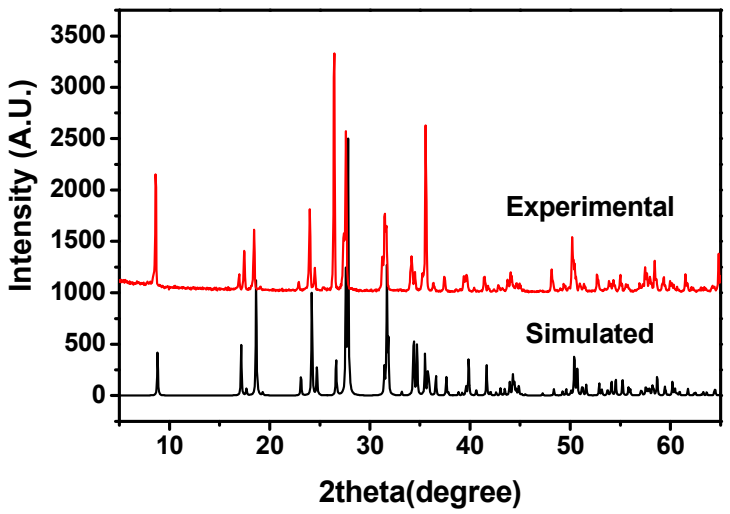

Figure S2. Experimental and simulated powder X-ray diffraction data for $Zn_2(VO_4)(IO_3)$.

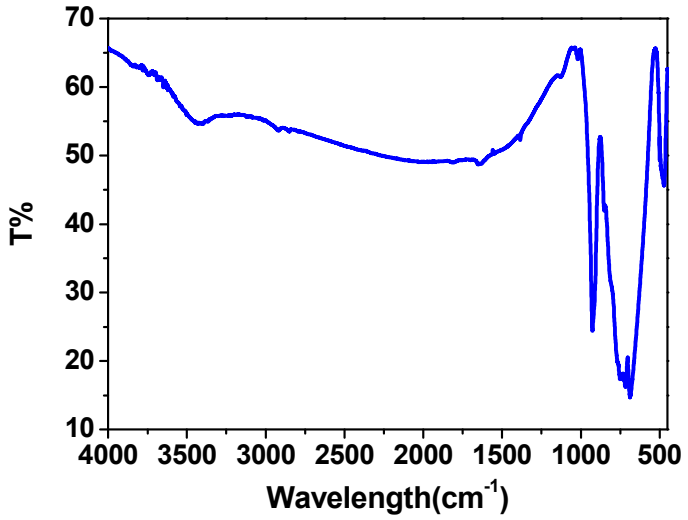

Figure S3. Infrared spectrum for $Zn_2(VO_4)(IO_3)$.

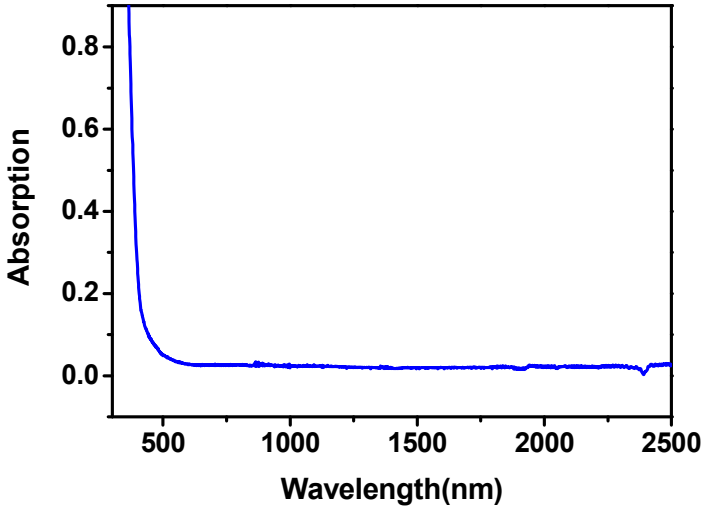

Figure S4. UV-Vis absorption spectrum for $Zn_2(VO_4)(IO_3)$.

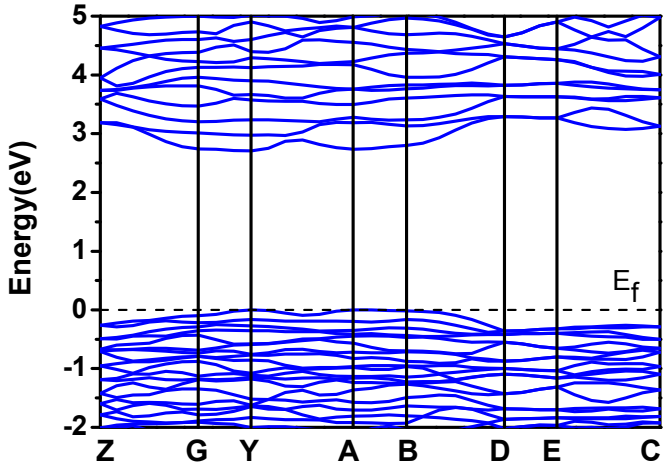

Figure S5. Calculated band structures of $Zn_2(VO_4)(IO_3)$ (the Fermi level is set at 0 eV).

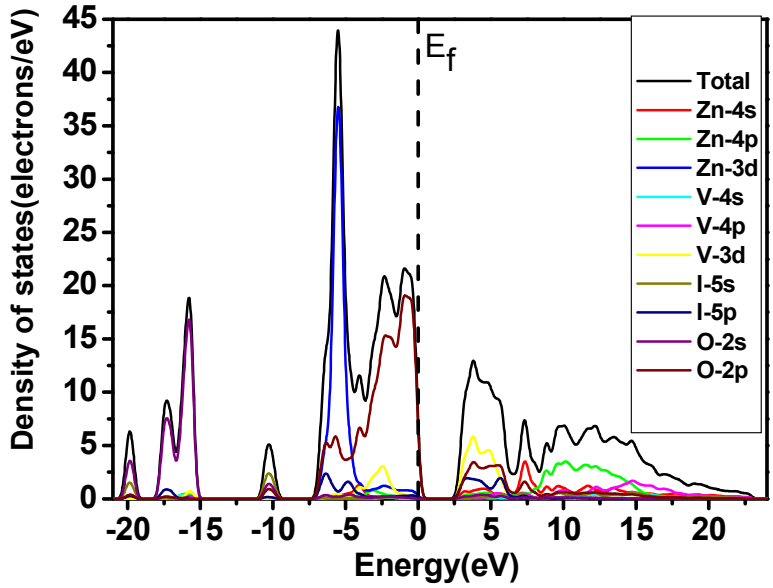

Figure S6. Total and partial electronic density of states of $Zn_2(VO_4)(IO_3)$.

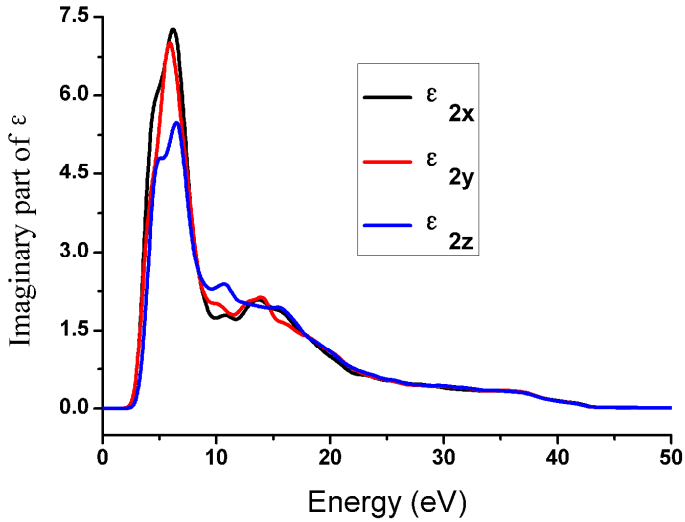

(a)

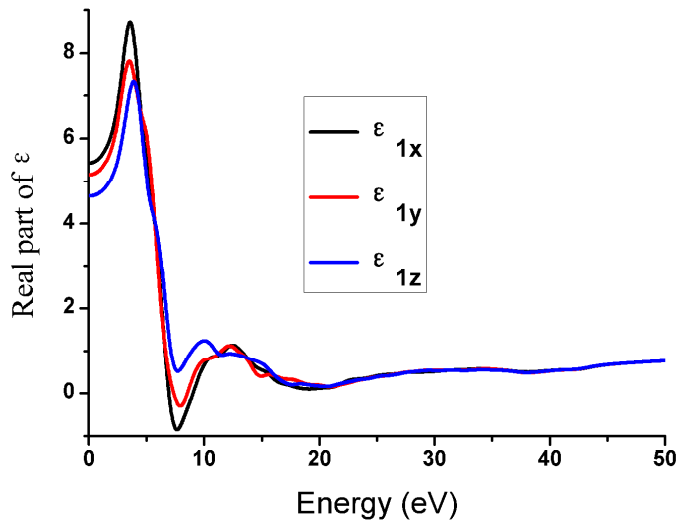

(b)

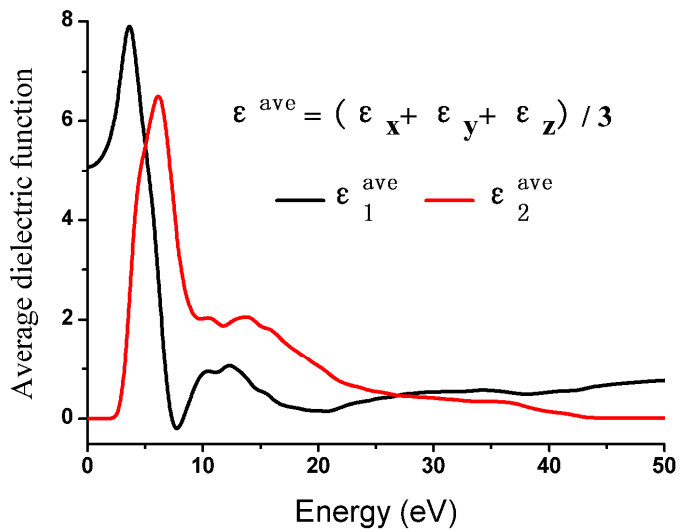

(c)

Figure S7. The imaginary and real parts of the dielectric function polarized along three dielectric axes directions (a and b) and the average imaginary part and real part of the dielectric function over three dielectric axes directions (c) for $Zn_2(VO_4)(IO_3)$.

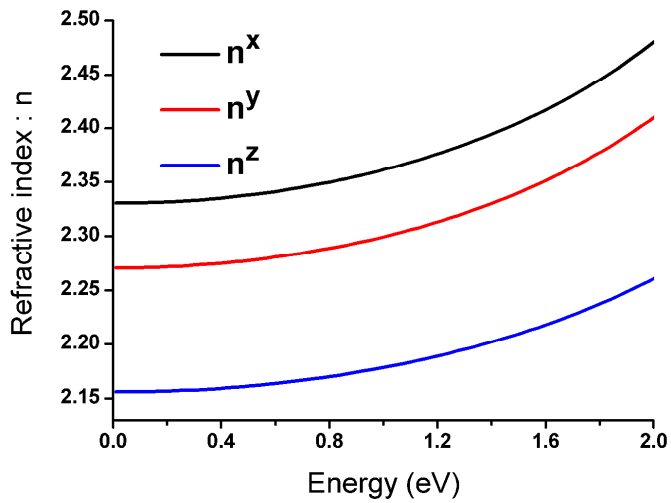

Figure S8. Calculated linear refractive indices for $Zn_2(VO_4)(IO_3)$.

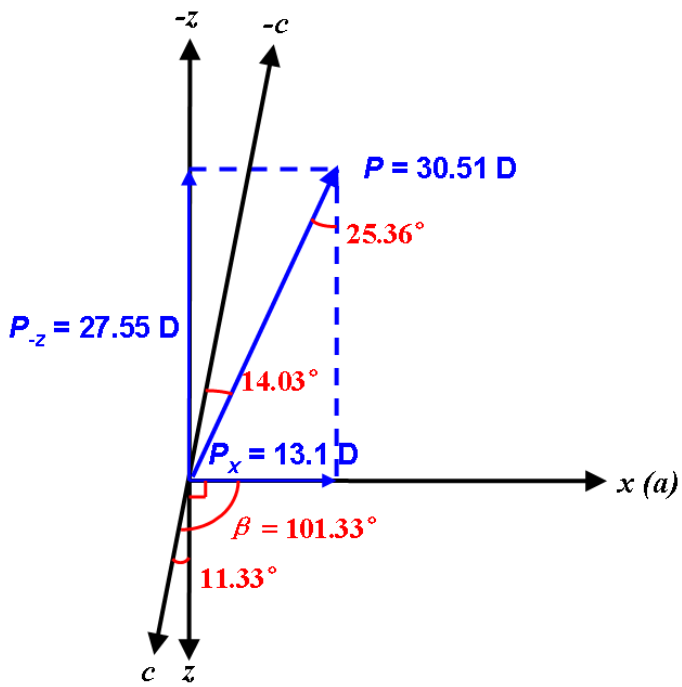

Figure S9. The calculated macroscopic dipole moment vector for $Zn_2(VO_4)(IO_3)$ (D = Debyes).